PHYSICAL REVIEW C **87**, 031601(R) (2013)

Ground-state and isomeric-state cross sections for ^{181}Ta(n, $2n$)^{180}Ta between 8 and 15 MeV

C. Bhatia,[1,2,*] M. E. Gooden,[2,3] W. Tornow,[1,2] and A. P. Tonchev[4]
[1]*Department of Physics, Duke University, Durham, North Carolina 27708, USA*
[2]*Triangle Universities Nuclear Laboratory, Durham, North Carolina 27708, USA*
[3]*Department of Physics, North Carolina State University, Raleigh, North Carolina 27695, USA*
[4]*Physics Division, Lawrence Livermore National Laboratory, Livermore, California 94550, USA*
(Received 8 January 2013; revised manuscript received 28 February 2013; published 21 March 2013)

Using the activation technique, the cross section for the reaction ^{181}Ta(n,2n)^{180}Ta^g was measured from 8 to 15 MeV in small energy steps to resolve inconsistencies in the existing database. The 93.4 keV γ ray from the decay of the ^{180}Ta^g ground state was recorded with a high-purity germanium (HPGe) detector. The monitor reactions ^{27}Al(n, α)^{24}Na and ^{197}Au(n,2n)^{196}Au were used for neutron fluence determination. The ENDF VII.1 and TENDL 2011 evaluations are in considerable disagreement with the present data, which in turn agree very well with the majority of the existing data in the 14 MeV energy region. A detailed analysis using the code TALYS was performed to describe the present data and to predict the (n,2n) cross section to the isomeric state of ^{180}Ta.

DOI: 10.1103/PhysRevC.87.031601 PACS number(s): 24.60.Dr, 25.40.Fq, 28.20.−v, 24.10.−i

Introduction. Tantalum plays an important role in nuclear fission and fusion applications [1]. For example, tantalum was used in the past as witness foils (chemical tracers) in underground tests of nuclear devices to assess their performance by recording the yield of the reaction ^{181}Ta(n,2n)^{180}Ta^g. More recently, in the design of accelerator driven systems, tantalum has been considered as the material of choice for the spallation target [2]. It is also important for future fusion reactors [3]. Very recently, the ^{181}Ta(n,2n)^{180}Ta^g reaction was viewed as an important diagnostic tool for studying and understanding the thermonuclear burn in the deuterium-tritium fuel capsule used in inertial confinement fusion research at the National Ignition Facility (NIF) at LLNL [4]. In addition, the isotope ^{180}Ta, often called the rarest isotope in the universe, has been subject of many fundamental physics studies due to the fact that it exists naturally only in its isomeric state. For the most part, this nucleus is bypassed by the major nucleosynthesis mechanisms of the s- and r-processes. That is the reason why this isotope has the lowest abundance of any stable nuclides. The reaction mechanisms leading to the isomeric or ground state of ^{180}Ta are of paramount importance for the understanding of the production of ^{180}Ta^m [5].

Unfortunately, the existing data for the ^{181}Ta(n,2n)^{180}Ta^g reaction cross section are inconsistent. In the well studied energy region around 14 MeV, the data can be grouped into two bands which differ by about 60%, as can be seen from Figs. 1(a) and 1(b). For example, the experimental data of Refs. [6–11] are clustered around cross-section values of 2200 mb, while the data of Refs. [12–26] are centered around 1300 mb. The ENDF VII.1 [27] and TENDL 2011 [28] evaluations favor the upper band. This group of data includes the most complete previous data set reported for the ^{181}Ta(n,2n)^{180}Ta^g reaction. These data were obtained by Frehaut *et al*. [8] by direct neutron detection, while the large majority of the data shown in Fig. 1 are based on the neutron activation technique. In view of this unsatisfactory situation and to provide more data below 12 MeV and closer to threshold than currently available, a new attempt was made to provide a definitive data set for the ^{181}Ta(n,2n)^{180}Ta^g reaction cross section in the 8 to 15 MeV energy range. This energy range is of special interest for applications as well as for nuclear astrophysics studies, and theoretical approaches aimed at calculating the ^{181}Ta(n,2n)^{180}Ta^m and ^{181}Ta(n,2n)^{180}Ta^g cross section at energies higher than studied in the present work.

Experimental procedure. The threshold energy for initiating the reaction ^{181}Ta(n,2n)^{180}Ta^g is 7.62 MeV. The ^{2}H(d,n)^{3}He reaction was used to produce quasi-monoenergetic neutrons between 8 and 14.5 MeV. Deuteron beams in the energy range between 5.3 and 11.9 MeV were provided by the Triangle Universities Nuclear Laboratory's (TUNL) tandem accelerator. Typical deuteron beam currents on target were 2 μA. The target consisted of a 3 cm long and 1 cm diameter cylindrical gas cell made of thin-walled stainless steel and filled with high-purity deuterium gas. A Havar foil of 6.35 μm thickness provided the seal to the accelerator vacuum. A 0.275 mm thick disk of tantalum served as beam stop. A schematic of the experimental setup is shown in Fig. 2. Depending on incident deuteron energy, the deuterium gas pressure was adjusted between 3 atm at the lowest energy and 4.6 atm at the highest energy to provide the desired neutron energy spread in the energy range investigated. Typically, the neutron energy spread was $\pm$120 keV at 0°. The uncertainty in the neutron energy scale is estimated to be $\pm$30 keV.

High-purity natural tantalum squares of 10 mm$\times$10 mm area and 0.125 mm thickness were attached to a low-mass holder and positioned 2.5 cm from the end of the deuterium gas cell at 0° relative to the incident deuteron beam direction (see Fig. 2). Due to the kinematics and the cross section of the ^{2}H(d,n)^{3}He reaction, this finite geometry decreases the nominal neutron energy and increases its energy spread. Using the cross section of Refs. [29,30], the effective mean neutron energy and its energy spread were calculated via Monte Carlo simulation. Numerical values are given in Table I. Depending

*Present address: Medical Physics and Applied Radiation Sciences, McMaster University, 1280 Main Street West, General Sciences Building, Hamilton, ON L8S 4K1, Canada; chitra@tunl.duke.edu.

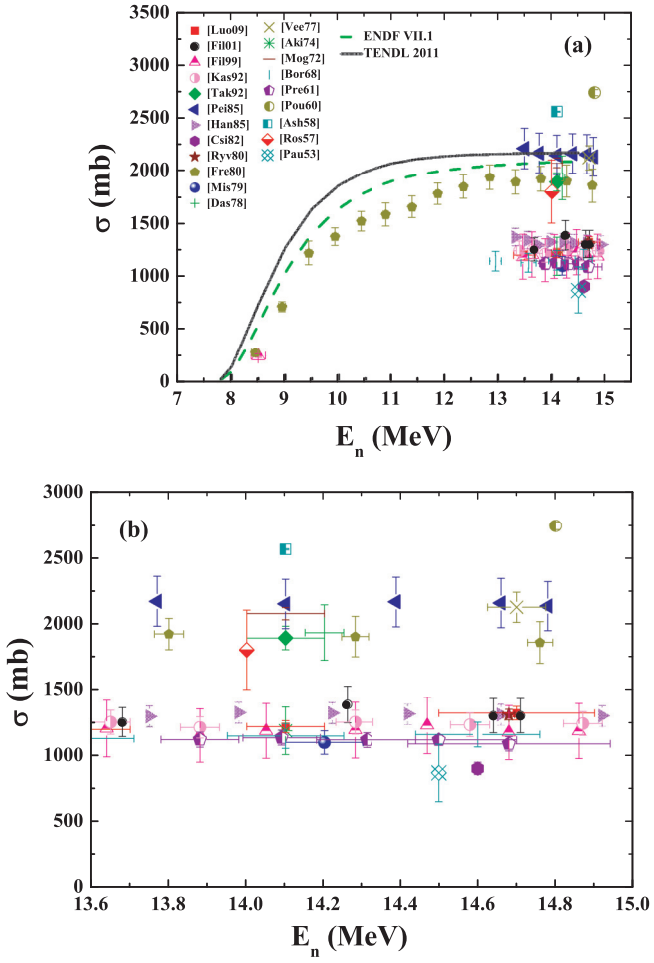

FIG. 1. (Color) (a) Existing angle-integrated cross-section data for the ^{181}Ta$(n, 2n)^{180}$Ta^g reaction [6–26] in comparison to the ENDF VII.1 [27] and TENDL 2011 [28] evaluations. (b) Expanded view of the energy region centered at 14 MeV.

on incident neutron energy, the tantalum squares were irradiated over a period of 6 to 12 hours with constant neutron flux of 4.4 $\times$ 10^6 to 2.9 $\times$ 10^7 s^{-1}. A 1.5 inch diameter $\times$1.5 inch long cylindrical BC501A [31] neutron detector placed 3 m downstream of the deuterium gas cell served as on-line neutron flux monitor. Simple reaction kinematics shows that lower energy neutrons from the deuteron breakup process on structural materials of the deuterium gas cell can initiate the

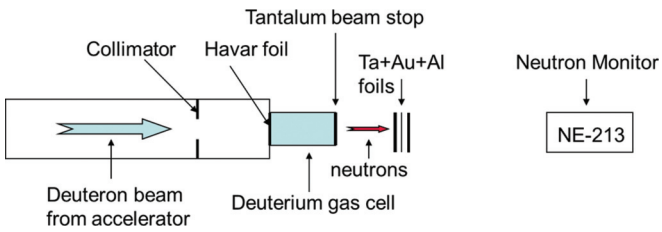

FIG. 2. (Color online) Schematic of experimental setup used for neutron activation measurements, consisting of a deuterium gas cell for the ^{2}H$(d,n)^3$He reaction, Ta, Au, and Al targets, and neutron monitor.

TABLE I. Summary of cross-section results for the reaction ^{181}Ta$(n,2n)^{180}$Ta^g. ΔE_n = neutron energy spread as explained in the text. $\Delta\sigma_1$ = statistical uncertainty. $\Delta\sigma_2$ = total uncertainty.

E_n (MeV)	$\pm\,\Delta E_n$	^{181}Ta$(n, 2n)^{180}$Ta^g		
		σ (mb)	$\Delta\sigma_1$	$\Delta\sigma_2$
7.93	0.20	27.06	0.40	1.36
8.18	0.19	97.44	0.84	4.51
8.43	0.19	154.40	1.10	7.20
8.93	0.20	404.61	1.30	21.59
9.43	0.20	723.28	2.90	33.60
9.91	0.24	862.74	3.20	46.05
10.91	0.23	1123.37	4.22	62.32
11.90	0.22	1206.11	5.45	55.85
12.90	0.22	1293.53	6.66	67.40
13.90	0.22	1189.25	7.95	61.56
14.39	0.22	1232.25	10.02	63.07
14.80	0.05	1233.70	11.56	60.57

^{181}Ta$(n,2n)$ ^{180}Ta^g reaction, if the incident deuteron energy is above about 9.8 MeV. This energy corresponds to neutron energies of above 12.5 MeV for the ^{2}H$(d,n)^3$He reaction, once the energy loss in the Havar foil is taken into account. Here, the breakup can take place on the entrance collimator (made of tantalum) of the deuterium gas cell, the Havar foil, and the tantalum beam stop. As a result, the contribution from the neutron continuum of the ^{2}H$(d,np)X$ breakup channel (here X stands for heavy elements) has to be considered for our three highest neutron energies of 12.9, 13.9, and 14.39 MeV. However, this effect is small and corrections were applied [32,33]. In addition, measurements were performed with an empty gas cell at E_n = 13 and 14.5 MeV. Here, the corrections were found to be about 2% and 5%, respectively. Neutrons from the deuteron breakup on the deuterium gas have energies below the ^{181}Ta$(n,2n)^{180}$Ta^g threshold, and therefore, do not contribute in the deuteron energy range used in the present work.

As an additional cross check of the procedure used above E_n = 12.5 MeV, the reaction ^{3}H$(d,n)^4$He was employed to produce 14.8 MeV neutrons. Here, a 2 Ci tritiated titanium target (see Ref. [34]) was used to take advantage of the large cross section at the 107 keV resonance. For this purpose, a 2 MeV deuteron beam from the tandem accelerator was energy degraded by a 6.35 μm Havar foil. In addition, the helium gas pressure (about 1.5 atm) in a small buffer cell located upstream of the tritiated target foil was fine tuned to maximize the neutron yield. This method was more convenient than changing the accelerator potential needed to adjust the incident deuteron energy to be centered on the narrow 107 keV resonance of the ^{3}H$(d,n)^4$He reaction.

The neutron fluence determination was accomplished by placing a gold (typically 44.6 mg) and an aluminum foil (typically 7.7 mg), each 10 mm $\times$ 10 mm in area and 0.025 mm in thickness, immediately downstream of the tantalum target foil (typically 0.225 g). The neutron activation cross sections for the reactions ^{197}Au$(n,2n)^{196}$Au and ^{27}Al$(n,\alpha)^{24}$Na were obtained from Ref. [35,36]. The threshold energy of the reaction ^{197}Au$(n,2n)^{196}$Au is only about 450 keV higher than

that of ^{181}Ta$(n,2n)^{180}$Ta^g. In addition, the ^{196}Au half-life time of $T_{1/2} = 6.17$ d and its deexcitation γ-ray energy of 355.7 keV with $I_\gamma = 0.87$ are very convenient features. As a result, the reaction ^{197}Au$(n,2n)^{196}$Au provides for an excellent absolute neutron fluence determination for the present work. The reaction ^{27}Al$(n,\alpha)^{24}$Na was used for $E_n < 12$ MeV only. In this energy regime, the fluence determined from the ^{197}Au$(n,2n)^{196}$Au and ^{27}Al$(n,\alpha)^{24}$Na reactions agreed within uncertainties, after small corrections were applied for low-energy neutrons in the latter case. Because of its threshold energy of 3.2 MeV, the ^{27}Al$(n,\alpha)^{24}$Na reaction is sensitive to breakup and room-return neutrons. Those effects have been studied and quantified in Refs. [37,38].

After irradiation, the Ta/Au/Al sample stack was placed at a distance of 5 cm in front of a 20% high-purity Germanium (HPGe) detector with the Ta foil facing the detector. This detector, located in TUNL's low-background counting facility, was well shielded against room and cosmic-ray background radiation. The efficiency and energy calibration of the detector were performed with the standard and well characterized radioactive sources ^{56}Co, ^{60}Co, ^{133}Ba, ^{137}Cs, and ^{152}Eu. The half-life time of ^{180}Ta^g is 8.154 h. The 93.4 keV γ-ray line originating from the electron capture (86%) to ^{180}Hf with $I_\gamma = 0.0451$ was used in the analysis. The 103.6 keV γ-ray line from the beta decay (14%) to ^{180}W with $I_\gamma = 0.0081$ was not used because of its larger statistical and branching uncertainties. A typical γ-ray spectrum is shown in Fig. 3. In addition to the three γ-ray lines at 93.4, 103.6, and 355.7 keV, the 1368.6 keV line from ^{24}Na is also indicated in Fig. 3. Background measurements with nonactivated Ta/Au/Al foils were performed to account for the environmental background line at $E_\gamma = 92.4$ keV, which originates from the β decay of ^{234}Th. After correcting for self-absorption in the Ta foil and coincidence summing (which turned out to be very small), decay curves were obtained, indicating good agreement between the measured and literature value for $T_{1/2}$. For the Au and Al foils, corrections were applied for γ-ray attenuation in the Ta foil, ranging from 1.05% to 1.01%, respectively.

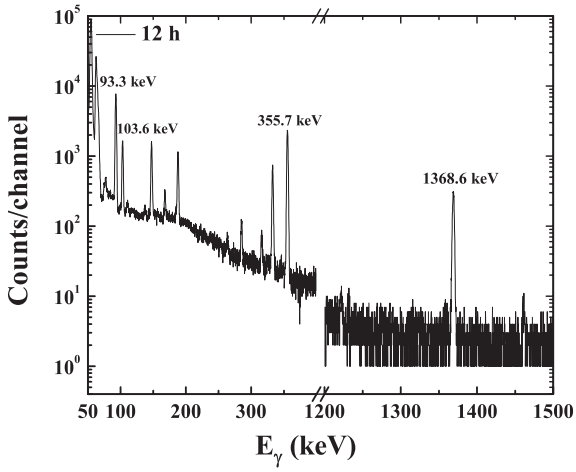

FIG. 3. Partial gamma-ray spectrum of ^{180}Ta^g obtained with a 20% efficient HPGe detector and recorded after twelve hours of neutron activation of ^{181}Ta at $E_n = 14.39$ MeV. The lines of interest are labeled.

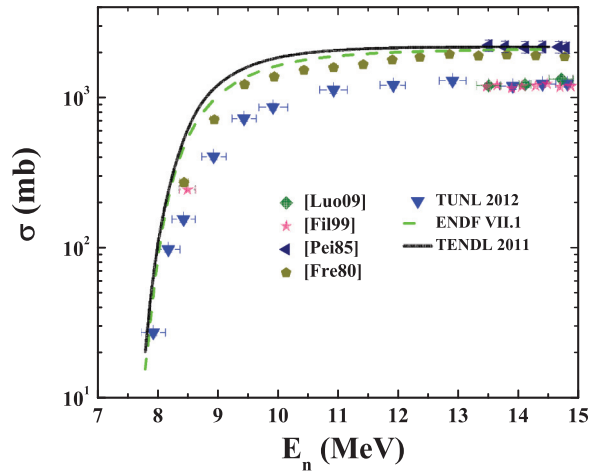

FIG. 4. (Color online) The present cross-section results obtained for the ^{181}Ta$(n,2n)^{180}$Ta^g reaction are shown by the upside-down triangles in comparison to a subset of previous measurements and recent evaluations.

The cross section of interest was obtained from the activation formula

$$A = \sigma\phi n(1 - e^{-\lambda t_i})e^{-\lambda t_d}(1 - e^{-\lambda t_c}),$$

where A is the number of decays per second, σ is the cross section in cm^2, ϕ is the incident neutron flux in n cm^{-2} s^{-1}, n is the number of target nuclei, t_i is the irradiation time, t_d is the decay time before the beginning of the offline γ-ray counting, t_c is the counting time, and finally λ is the decay constant.

Results and discussion. Figure 4 shows the measured cross-section data (upside-down triangles) between 7.9 and 14.8 MeV in comparison to the data of Frehaut *et al*. [8] (solid pentagons), and some of the data [6–26] between 12 and 14.8 MeV already shown in Fig. 1. Our data are in striking disagreement with the former data set, which has been the most complete data set available for the reaction ^{181}Ta$(n,2n)^{180}$Ta^g before the present data were obtained. However, in the 12 to 14.8 MeV energy range, our data are in excellent agreement with the majority of the data belonging to the lower band shown in Fig. 1. It should be noted that the disagreement with the data of Frehaut *et al*. [8] found in the present work is especially troublesome in view of Ref. [39], which states that the cross-section values reported by Frehaut *et al*. [8] were in fact too low by about 10%. As a result, the recent evaluation by Pereslavtsev and Fischer [40] overestimates the ^{181}Ta$(n,2n)^{180}$Ta^g cross section at 14 MeV by about 80% compared to our work.

As can be seen in Fig. 4, the present data are in stark disagreement with the Evaluated Nuclear Data File (ENDF) VII.1 [27] and TENDL [28] evaluations, which favor the upper band. Our data below 9 MeV were deconvoluted to correct for the strong energy dependence of the measured data. Using a trial function (based on past experience) for the energy dependence of the cross section, the experimental setup was simulated via Monte Carlo technique. Here, the differential neutron-production cross sections of Refs. [29,30] were used.

TABLE II. Sources and approximate magnitudes of the uncertainties (in%) in the present cross-section measurement.

Uncertainty	Magnitude (%)
Statistics	1–1.5
Sample mass	<1
Detector efficiency	2–3
Branching ratio	3.5
Product half-life	⩽0.5
Monitor cross section	1–2 (Al)
	1–3 (Au)
Low-energy neutrons	<1
Total[a]	4.4–5.9

[a]Total uncertainty obtained from individual uncertainties added in quadrature.

Typically, after one iteration the modified trial function was in agreement with the experimental data.

Tables I and II present the cross-section results and the error budget, respectively. As shown in Table II, the overall uncertainty is governed by the sizeable uncertainty in the branching value I_γ for the 93.4 keV transition.

TALYS *calculations*. Figure 5 shows a TALYS calculation [41]. Parameters such as resonances, level density, discrete levels, and γ-ray strength function were varied within the recommended values of the RIPL-2 database [42]. It was found, as expected, that the calculation was mostly sensitive to the nuclear level density and the nuclear structure of the nucleus. Only the level density parameter was adjusted from the RIPL-2 recommended value of 20.28 MeV to 21.92 MeV to reproduce the present data. The other parameters such as nuclear masses, ground-state deformation, and discrete levels were taken from the literature systematic [42] for reasons of consistency. This parameter set was then used to generate cross-section results for all open reaction channels, including the $(n,2n)$ channel to the isomeric state as well as to the ground state of ^{180}Ta. The default optical-model potentials were used to calculate the reaction cross sections and the total cross section. Moreover, TALYS yields the transmission coefficients for compound nucleus calculations and all cross sections and angular distributions for discrete states. The reaction mechanism, compound or direct, is calculated based on the Hauser-Feshbach formalism including width fluctuation corrections, which accounts for the correlation between the incident and outgoing waves. Because the projectile energy is above the particle-emission threshold of competing open channels, the width fluctuation correction factor is negligible in all methods implemented in TALYS, and the simple Hauser-Feshbach model is adequate to describe the compound-nucleus decay. The nuclear level density was fitted to properly reproduce the known s-wave resonance spacing ($D_0 = 1.2$ eV) at the neutron capture energy and also to reproduce the cumulative numbers of known low-lying states. The new energy-, spin-, and parity-dependent nuclear level densities based on the microscopic combinatorial [43] provide the best fit to the experimental data (see short-dashed curve in Fig. 5). The other level-density models such as back-shifted Fermi gas, constant temperature, and generalized super-fluid models predict larger $(n,2n)$ cross-section values below 10 MeV.

As a by-product, for incident neutron energies of 13 MeV and above, cross-section data for the reactions ^{181}Ta$(n,p)^{181}$Hf^g and ^{181}Ta$(n,d)^{180}$Hf^m were obtained in the present work. These data are in good agreement with the present TALYS calculations, as can be seen in Fig. 6. The (n,p) data also agree reasonably well with the data of Ref. [12]. It is interesting to point out that the (n,p) and (n,d) cross-section data of ^{181}Ta^g are a factor of 300 and 6000, respectively, smaller than the $(n,2n)$ reaction cross section.

It is of special interest to study the reaction cross section to the isomeric state ($J^\pi = 9^-$) of ^{180}Ta after the statistical-model calculations to the ground state were constrained. The half-life time of the isomeric state is $T_{1/2} \geqslant 10^{15}$ years, and measuring the ^{181}Ta$(n,2n)^{180}$Ta^m reaction cross section leading to this

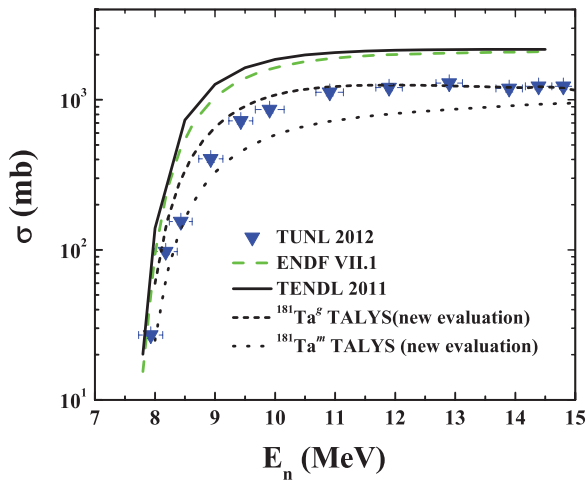

FIG. 5. (Color online) TALYS calculations [41] (short-dashed and dotted curves) with parameters adjusted to reproduce the present data, in comparison to the ENDF VII.1 [27] and TENDL 2011 [28] evaluations.

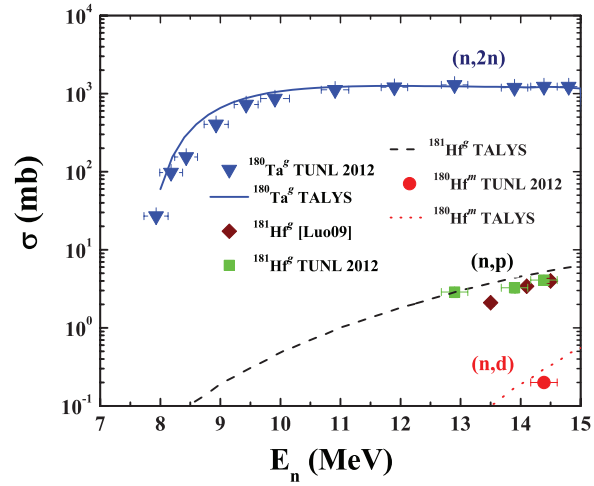

FIG. 6. (Color online) Present cross-section data for ^{181}Ta$(n,2n)^{180}$Ta^g, ^{181}Ta$(n,p)^{181}$Hf^g, and ^{181}Ta$(n,d)^{180}$Hf^m reactions in comparison to TALYS [41] calculations and Luo *et al.* [12] in the case of ^{181}Ta$(n,p)^{181}$Hf^g.

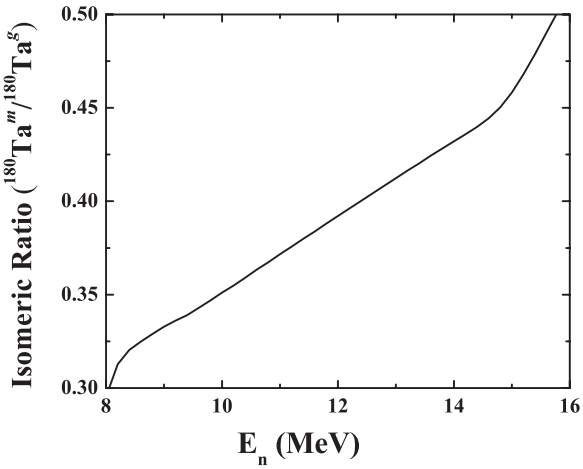

FIG. 7. Isomeric cross-section ratio ^{180}Ta^m/^{180}Ta^g calculated using TALYS [41].

state remains an experimental challenge. Because of the large spin difference between the isomeric and ground state ($\Delta J = 8$), and the absence of levels located below the isomeric state with adjacent spin values, ^{180}Ta^m is a classical example of a "spin-trap" isomer. The calculated cross section for the reaction ^{181}Ta$(n,2n)^{180}$Ta^m is shown in Fig. 5 (dotted curve) in comparison to the ground-state cross section and its associated evaluations. Despite the large spin difference between the isomeric and the ground states, the isomeric cross-section ratio ^{180}Ta^m/^{180}Ta^g, for example at 14.5 MeV, is 44% as shown in Fig. 7. According to our knowledge, this is the largest isomeric ratio found for any $(n,2n)$ reaction with spin difference of $\Delta J = 8$.

Conclusions. We propose to adopt the present TALYS calculations in the 10 to 15 MeV energy range as the new recommended evaluations for the ^{181}Ta$(n,2n)^{180}$Ta^g and ^{181}Ta$(n,2n)^{180}$Ta^m cross section. Below 10 MeV the present data are lower in magnitude than the TALYS calculations. An unexpectedly large cross section is predicted by the TALYS calculations for the $(n,2n)$ reaction to the ^{180}Ta^m isomeric state.

Acknowledgment. The authors acknowledge valuable contributions from M. Bhike, S. W. Finch, C. R. Howell, J. H. Kelley, J. B. Wilhelmy, and D. J. Vieira. Fruitful discussions with S. Goriely are gratefully acknowledged. This work was supported in part by the National Nuclear Security Administration under the Stewardship Science Academic Alliance Program through the US Department of Energy Grant No. DE-FG52-09NA29465.

[1] V. Avrigeanu, S. V. Chuvaev, R. Eichin *et al.*, Nucl. Phys. A **765**, 1 (2006).
[2] G. S. Bauer, Nucl. Instrum. Methods Phys. Res. A **463**, 505 (2001).
[3] V. Shankar *et al.*, Fusion Eng. Des. **87**, 318 (2012).
[4] P. A. Bradley, G. P. Grim, A. C. Hayes *et al.*, Phys. Rev. C **86**, 014617 (2012).
[5] P. Mohr, F. Kappeler, and R. Gallino, Phys. Rev. C **75**, 012802(R) (2007).
[6] A. Takahashi *et al.*, Osaka University OKTAVIAN Report No. 92, 1992 (unpublished), p. 01.
[7] F. Peiguo *et al.*, Chin. J. Nucl. Physics (Beijing) **7**, 242 (1985).
[8] J. Frehaut, A. Bertin, R. Bois, and J. Jary, in International Symposium on Neutron Cross Sections from 10 to 50 MeV, Upton, New York, 1980 (unpublished), p. 399.
[9] L. R. Veeser, E. D. Arthur, and P. G. Young, Phys. Rev. C **16**, 1792 (1977).
[10] A. Poularikas *et al.*, J. Inorg. Nucl. Chem. **13**, 196 (1960).
[11] V. J. Ashby *et al.*, Phys. Rev. **111**, 616 (1958).
[12] J. Luo, F. Tuo, and X. Kong, Phys. Rev. C **79**, 057603 (2009).
[13] A. A. Filatenkov and S. V. Chuvaev, Khlopin Radium Institute, Leningrad, Report No. 258, 2001 (unpublished).
[14] A. A. Filatenkov *et al.*, Khlopin Radium Institute, Leningrad, Report No. 252, 1999 (unpublished).
[15] Y. Kasugai *et al.*, JAERI-M Report No. 93046, 1992 (unpublished), p. 277.
[16] L. Hanlin, Z. Wenrong, and Fan Peiguo, Nucl. Sci. Eng. **90**, 304 (1985).
[17] J. Csikai, in *Proceedings of the International Conference on nuclear Data for Science and Technology*, Antwerpen, 1982 (unpublished), p. 414.
[18] T. B. Ryves and P. Kolkowski, J. Phys. G: Nucl. Part. Phys. **6**, 771 (1980).
[19] S. C. Misra and U. C. Gupta, J. Phys. G: Nucl. Part. Phys. **5**, 855 (1979).
[20] N. Lakshmana Das *et al.*, Nuovo Cimento A **48**, 500 (1978).
[21] T. Akiyoshi *et al.*, J. Nucl. Sci. Technol. **11**, 523 (1974).
[22] R. Mogharrab and H. Neuert, Atomkernenergie **19**, 107 (1972).
[23] M. Bormann *et al.*, Nucl. Phys. A **115**, 309 (1968).
[24] R. J. Prestwood and B. P. Bayhurst, Phys. Rev. **121**, 1438 (1961).
[25] L. Rosen and L. Stewart, Phys. Rev. **107**, 824 (1957).
[26] E. B. Paul and R. L. Clarke, Can. J. Phys. **31**, 267 (1953).
[27] M. B. Chadwick, M. Herman, P. Oblozinsky *et al.*, Nucl. Data Sheets **112**, 2887 (2011).
[28] http://www.talys.eu/tendl/
[29] H. Liskien and A. Paulsen, Nucl. Data Tables **11**, 569 (1973).
[30] M. Drosg, http://homepage.univie.ac.at/manfred.drosg/Drosg2000.html
[31] D. E. Gonzalez Trotter, F. Salinas Meneses, W. Tornow *et al.*, Nucl. Instrum. Methods Phys. Res. **599**, 234 (2009); http://www.detectors.saint-gobain.com
[32] R. Raut *et al.*, Phys. Rev. C **83**, 044621 (2011).
[33] A. P. Tonchev *et al.*, Phys. Rev. C **77**, 054610 (2008).
[34] C. Bhatia, S. W. Finch, M. E. Gooden, and W. Tornow, Phys. Rev. C **87**, 011601(R) (2013).
[35] K. I. Zolotarev, INDC Report No. (NDS)-0526, 2008 (unpublished).
[36] K. I. Zolotarev, INDC Report No. (NDS)-0546, 2009 (unpublished).
[37] Y. Kasugai *et al.*, Ann. Nucl. Energy **25**, 23 (1998).
[38] R. Macri *et al.*, LLNL-TR-533294 (2012).
[39] H. Vonach, A. Pavlik, and B. Strohmaier, Nucl. Sci. Eng. **106**, 409 (1990).

[40] P. Pereslavtsev and U. Fischer, Nucl. Instrum. Methods Phys. Res. B **248**, 225 (2006).

[41] A. Koning, S. Hillaire, and M. C. Duijvestijn, in *International Conference on Nuclear Data for Science and Technology*, Santa Fe, 2004, edited by R. C. Haight, M. B. Chadwick, T. Kawano, and P. Talou, AIP Conf Proc. No. 769 (AIP, New York, 2005), p. 1154.

[42] http://wwwnds.iaea.or.at/RIPL-2.

[43] S. Goriely, S. Hilaire, and A. J. Koning, Phys. Rev. C **78**, 064307 (2008).